

Eur. Phys. J. A **36**, 1–5 (2008)  
DOI 10.1140/epja/i2007-10554-7

THE EUROPEAN  
PHYSICAL JOURNAL A

Letter

## Letter

# A study of the proton resonant property in $^{22}\text{Mg}$ by elastic scattering of $^{21}\text{Na} + p$ and its astrophysical implication in the $^{18}\text{Ne}(\alpha, p)^{21}\text{Na}$ reaction rate

J.J. He<sup>1,a</sup>, S. Kubono<sup>1</sup>, T. Teranishi<sup>2</sup>, M. Notani<sup>1,b</sup>, H. Baba<sup>1</sup>, S. Nishimura<sup>3</sup>, J.Y. Moon<sup>4</sup>, M. Nishimura<sup>3</sup>, S. Michimasa<sup>1</sup>, H. Iwasaki<sup>3</sup>, Y. Yanagisawa<sup>3</sup>, N. Hokoïwa<sup>2</sup>, M. Kibe<sup>2</sup>, J.H. Lee<sup>4</sup>, S. Kato<sup>5</sup>, Y. Gono<sup>2</sup>, and C.S. Lee<sup>4</sup>

<sup>1</sup> Center for Nuclear Study, University of Tokyo (CNS), Wako Branch, 2-1 Hirosawa, Wako, Saitama 351-0198, Japan

<sup>2</sup> Department of Physics, Kyushu University, 6-10-1 Hakozaki, Fukuoka 812-8581, Japan

<sup>3</sup> RIKEN (The Institute of Physical and Chemical Research), 2-1 Hirosawa, Wako, Saitama 351-0198, Japan

<sup>4</sup> Department of Physics, Chung-Ang University, Seoul 156-756, Republic of Korea

<sup>5</sup> Department of Physics, Yamagata University, Yamagata 990-8560, Japan

Received: 18 October 2007 / Revised: 13 February 2008

Published online: 3 April 2008 – © Società Italiana di Fisica / Springer-Verlag 2008

Communicated by E. Bellotti

**Abstract.** Proton resonances in  $^{22}\text{Mg}$  have been investigated by the resonant elastic scattering of  $^{21}\text{Na} + p$ . The  $^{21}\text{Na}$  beam with a mean energy of 4.00 MeV/nucleon was separated by the CNS radioactive-ion-beam separator (CRIB) and bombarded a thick  $(\text{CH}_2)_n$  target. The energy spectra of recoiled protons were measured at scattering angles of  $\theta_{c.m.} \approx 172^\circ, 146^\circ$ , respectively. Several excited states observed before have been confirmed including two states (at 6.616, 6.796 MeV) observed at TRIUMF. A new state at 7.06 MeV has been observed, and another new one at 7.28 MeV is tentatively identified due to its low statistics. The proton resonant parameters were deduced from an  $R$ -matrix analysis of the differential cross-section data with a SAMMY-M6-BETA code. The astrophysical implication for the  $^{18}\text{Ne}(\alpha, p)^{21}\text{Na}$  reaction has been briefly discussed.

**PACS.** 25.60.-t Reaction induced by unstable nuclei – 23.50.+z Decay by proton emission – 26.50.+x Nuclear physics aspects of novae, supernovae, and other explosive environments

## 1 Introduction

The structure of  $^{22}\text{Mg}$  has received great interest in recent years because of its important role in determining the astrophysical reaction rates of  $^{21}\text{Na}(p, \gamma)^{22}\text{Mg}$  and  $^{18}\text{Ne}(\alpha, p)^{21}\text{Na}$  reactions in explosive stellar scenarios [1, 2].

The excited states in  $^{22}\text{Mg}$  have been investigated via many reactions; the  $^{24}\text{Mg}(p, t)^{22}\text{Mg}$  [3–6],  $^{24}\text{Mg}(^4\text{He}, ^6\text{He})$  [7] and  $^{12}\text{C}(^{16}\text{O}, ^6\text{He})$  reactions [8], which preferentially populate the natural-parity states in  $^{22}\text{Mg}$ ; the  $^{25}\text{Mg}(^3\text{He}, ^6\text{He})$  reaction [9] which populates both the natural-parity and unnatural-parity states; the

$^{20}\text{Ne}(^3\text{He}, n)$  reaction [10, 11] as well as the  $^{20}\text{Ne}(^3\text{He}, n\gamma)$  reaction [12, 13]. By knowing the location of excitation states in  $^{22}\text{Mg}$ , the resonance property of states just above the proton threshold has been studied by the direct  $^{21}\text{Na}(p, \gamma)^{22}\text{Mg}$  measurements [14, 15] as well as by a resonant scattering measurement of  $^{21}\text{Na} + p$  [16] with the DRAGON recoil separator at TRIUMF.

The astrophysical implication of the  $^{21}\text{Na}(p, \gamma)^{22}\text{Mg}$  reaction has been discussed on a firm experimental result [15]. The conclusion is that the resonance at  $E_x = 5.714$  MeV dominates the  $^{21}\text{Na}(p, \gamma)^{22}\text{Mg}$  rate up to temperatures 1.1 GK, and the contributions from the resonances at  $E_x = 6.246, 6.329$  MeV become dominant beyond that temperature. Finally, Seweryniak *et al.* [17] have concluded that no further measurement is needed to determine this resonant reaction rate under nova conditions.

In another aspect, Wiescher *et al.* [1] have proposed that the  $^{18}\text{Ne}(\alpha, p)^{21}\text{Na}$  reaction is probably one of the key reactions for the break-out from the hot CNO cycle

<sup>a</sup> Present address: School of Physics, University of Edinburgh, Mayfield Road, Edinburgh, EH9 3JZ, UK; e-mail: [hjianjun@ph.ed.ac.uk](mailto:hjianjun@ph.ed.ac.uk)

<sup>b</sup> Present address: Argonne National Laboratory, 9700 S. Cass Avenue, Argonne, IL 60439, USA.

in X-ray burst. In order to estimate the resonant reaction rate of  $^{18}\text{Ne}(\alpha, p)^{21}\text{Na}$ , the knowledge about the resonant properties of those states above the  $\alpha$  threshold ( $Q = 8.14\text{ MeV}$ ) in  $^{22}\text{Mg}$  is required. The resonant property of those states at  $E_x = 10.12\text{--}11.13\text{ MeV}$  has been studied via the direct  $^{18}\text{Ne}(\alpha, p)^{21}\text{Na}$  measurement [18,19], but the observed states are too high in energy for nucleosynthesis. As for the states above the  $\alpha$  threshold, although their excitation energies were determined [7–9,11], their resonant properties (such as,  $J^\pi$ ,  $\Gamma_\alpha$  and  $\Gamma_p$ ) have not been determined yet. Actually, in calculating the resonant reaction rate of  $^{18}\text{Ne}(\alpha, p)^{21}\text{Na}$  using the narrow resonance formalism, the knowledge of the proton partial widths ( $\Gamma_p$ ) is not required, since the resonance strength depends on the factor  $\frac{\Gamma_\alpha \Gamma_p}{\Gamma_{tot}}$  and is based on the knowledge of the states in  $^{22}\text{Ne}$ ,  $\Gamma_\alpha \ll \Gamma_p \approx \Gamma_{tot}$ , so that  $\omega\gamma = (2J+1)\Gamma_\alpha$ , where  $J$  is the spin of the resonant states, and the partial width  $\Gamma_\alpha$  is given by  $\Gamma_\alpha = \frac{3\hbar^2}{\mu R^2} P_l C^2 S_\alpha$  [8,20]. The spectroscopic  $S_\alpha$  factors were assumed from those of mirror states by Görres *et al.* [20] based on the  $^{18}\text{O}(^6\text{Li}, d)^{22}\text{Ne}$   $\alpha$ -transfer studies [21]. Therefore, the spin-parity of the resonance and the uncertainty in  $S_\alpha$  caused by the potential incorrectness of mirror assignments are still unknown.

This letter reports the resonant properties of the states in  $^{22}\text{Mg}$ , covering  $E_x = 6.6\text{--}8.7\text{ MeV}$ , by using the resonant elastic scattering of a  $^{21}\text{Na}$  beam on a thick  $(\text{CH}_2)_n$  target. The resonant properties have been determined by an  $R$ -matrix analysis of the differential elastic-scattering cross-sections of  $^{21}\text{Na} + p$ . The astrophysical implication for the  $^{18}\text{Ne}(\alpha, p)^{21}\text{Na}$  reaction has been discussed based on the present work.

## 2 Experiment and results

The experiment was performed using the CNS radioactive-beam separator (CRIB) [22,23]. An  $8.11\text{ A MeV}$   $^{20}\text{Ne}^{8+}$  beam bombarded a water-cooled  $^3\text{He}$  gas target ( $0.36\text{ mg/cm}^2$ ), where a  $^{22}\text{Mg}$  beam was produced by the  $^3\text{He}(^{20}\text{Ne}, ^{22}\text{Mg})n$  reaction, and simultaneously a  $^{21}\text{Na}$  beam was produced probably through  $^3\text{He}(^{20}\text{Ne}, ^{22}\text{Mg}^*)n$  with subsequent decay to  $^{21}\text{Na} + p$ . Both  $^{21}\text{Na}$  and  $^{22}\text{Mg}$  radioactive ions have been separated from the contaminants and utilized in the experiment. The results relevant to the application of the  $^{22}\text{Mg}$  beam have been published elsewhere [24].

The radioactive  $^{21}\text{Na}$  beam, with a mean energy of  $4.00\text{ MeV/nucleon}$  ( $4.1\%$  in FWHM) and an average intensity of  $1.5 \times 10^4$  particles/s, was delivered at the secondary target position where it bombarded a  $7.9\text{ mg/cm}^2$   $(\text{CH}_2)_n$  foil in which the  $^{21}\text{Na}$  particles were stopped. The recoiled light particles were measured using the  $\Delta E$ - $E$  Si telescopes that subtended  $\Delta\theta_{lab} \simeq 10^\circ$  ( $\sim 35\text{ m sr}$  in solid angle). The energy calibration for the detector system was performed using the secondary proton beams separated by CRIB at several energy points. In addition, a carbon target with a stopping thickness equivalent to that of the  $(\text{CH}_2)_n$  target was used in a separate run for evaluating the background contribution.

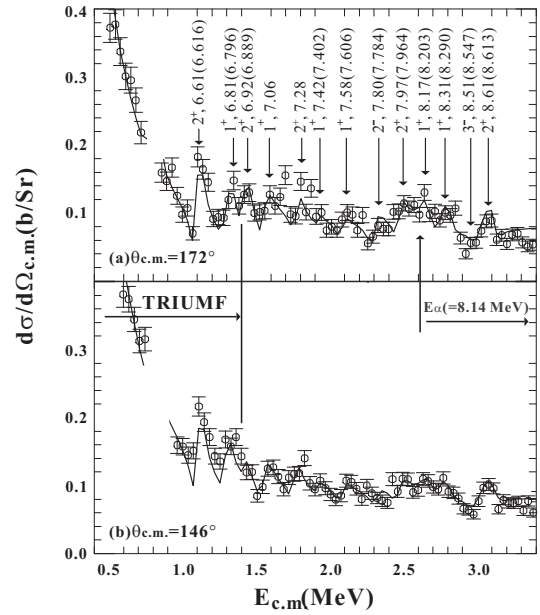


**Fig. 1.**  $R$ -matrix analysis of center-of-mass differential cross-sections for the  $^{21}\text{Na}+p$  resonant elastic scattering at the angles of (a)  $\theta_{c.m.} \approx 172^\circ$ , and (b)  $\theta_{c.m.} \approx 146^\circ$ . See text for details.

The center-of-mass energy ( $E_{c.m.}$ ) has been deduced using the elastic-scattering kinematics of  $^{21}\text{Na}+p$  with correction of the energy loss of particles in the target. At the scattering angle of  $\theta_{c.m.} \approx 172^\circ$ , the typical energy resolution (FWHM of  $E_{c.m.}$ ) is approximately  $20\text{ keV}$  at  $E_{c.m.} = 0.5\text{ MeV}$  and  $45\text{ keV}$  at  $E_{c.m.} = 3.5\text{ MeV}$ , and the corresponding energy uncertainty is approximately  $\pm 15\text{ keV}$  and  $\pm 20\text{ keV}$ , respectively; at  $\theta_{c.m.} \approx 146^\circ$ , the typical energy resolution is approximately  $20\text{ keV}$  at  $E_{c.m.} = 0.5\text{ MeV}$  and  $75\text{ keV}$  at  $E_{c.m.} = 3.5\text{ MeV}$ , and the corresponding energy uncertainty is approximately  $\pm 15\text{ keV}$  and  $\pm 30\text{ keV}$ , respectively. The major contributions in resolution and uncertainty of the  $E_{c.m.}$  energy to the latter telescope are from two aspects, one is the large kinematical shift, and the other one is that, for this position-sensitive detector, only horizontal  $x$  strips were used and vertical  $y$  strips were unused due to practical difficulties.

Figures 1 (a) and (b) show the center-of-mass differential cross-sections for the  $^{21}\text{Na} + p$  elastic scattering at angles of  $\theta_{c.m.} \approx 172^\circ$  and  $146^\circ$ , respectively. The cross-section data have been corrected for the stopping cross-sections [25], and the data within the dead layer region (between  $\Delta E$  and  $E$ ) were removed from the figures. The excitation energies indicated on the figure are calculated by the relation  $E_x = E_r + 5.502\text{ MeV}$ , where the resonant energies  $E_r$  are deduced from the  $R$ -matrix analysis, and the previously determined ones are shown in parentheses for comparison. The region investigated by the TRIUMF group is also indicated, and two resonant states well observed at  $E_x = 6.61, 6.81\text{ MeV}$  are corresponding to the previously observed  $6.615, 6.795\text{ MeV}$  states, respectively [16].

The c.m. differential cross-sections have been analyzed by an  $R$ -matrix [26] code SAMMY-M6-BETA [27], which

**Table 1.** Resonant properties of excited states in  $^{22}\text{Mg}$  deduced from the present work. The excitation energies from the previous work are listed for comparison. The uncertainties of energy, in units of keV, are included in the parentheses. The proton partial widths are deduced from the  $R$ -matrix analysis with those spin-parity assignments as shown in fig. 1.

$E_x^{\text{present}}$	$E_x$ [7]	$E_x$ [8]	$E_x$ [9]	$E_x$ [11]	Parity <sup>a</sup>	$J^\pi$ ( $R$ -matrix) <sup>b</sup>	$J^\pi; \ell$ (adopted)	$\Gamma_p$ (keV)
6.61(15) <sup>c</sup>	6.606(9)	6.606(11)	6.616(4)		$\pi = \text{N}$ [4]	$(2^+, 1^+)$	$2^+; 0$	23(7)
6.81(15) <sup>d</sup>	6.766(12)	6.767(20)	6.771(5)	6.760(90)		$(1^+, 2^+)$	$(1^+, 2^+); 0$	62(7)
6.92(15)		6.889(10)	6.878(9)		$\pi = \text{N}$	$(2^+, 1^+, 3^-, 2^-)$	$(2^+, 3^-); 0(1)$	16(7)
7.06(16)						$(1^+, 3^-, 2)$	$(1^+, 3^-, 2); 0(1)$	48(7)
7.28(16)						$(2^+, 1^+)$	$(2^+, 1^+); 0$	17(7)
7.42(17)		7.402(13)	7.373(9)			$(1, 2^+)$	$(1, 2^+); 0(1)$	10(7)
7.58(17)	7.614(9)		7.606(11)			$(1^+, 2^+)$	$(1^+, 2^+); 0$	23(7)
7.80(18)		7.784(18)	7.757(11)	7.840(90)	$\pi = \text{uN}$	$(1^- - 3^-)$	$(2^-); 1$	27 <sup>g</sup>
7.97(19)	7.938(9)	7.964(16)	7.986(16)	7.890(100)	$\pi = \text{N}$	$(1^+, 2^+)$	$(2^+); 0$	20 <sup>g</sup>
8.17(19)	8.197(10)	8.203(23)	8.229(20)			$(1^+ - 3^+)$	$(1^+ - 3^+); 2$	34 <sup>g</sup>
8.31(20)				8.290(40)		$(1^+ - 3^+)$	$(1^+ - 3^+); 2$	53 <sup>g</sup>
8.51(20) <sup>e</sup>	8.512(10)	8.547(18)		8.550(90)	$\pi = \text{N}$	$(1^- - 3^-)$	$(3^-); 1$	40(7)
8.61(21) <sup>f</sup>	(8.644(18))	8.613(20)	8.598(20)			$(2^+)$	$(2^+); 2$	27(7)

<sup>a</sup> N, uN denote the level of natural and unnatural parity, respectively.

<sup>b</sup> Present results deduced from the  $R$ -matrix analysis.

<sup>c</sup>  $J^\pi = 2^+$  determined for the 6.616 MeV state [16].

<sup>d</sup>  $J^\pi = (1^-, 2^-)$  determined for the 6.796 MeV state [16].

<sup>e</sup>  $J^\pi = 2^+$  assumed in Chen *et al.* [8].

<sup>f</sup>  $J^\pi = 3^-$  assumed in Chen *et al.* [8].

<sup>g</sup> The proton widths of these states are only roughly estimated from the  $R$ -matrix fits on the data.

enables multilevel  $R$ -matrix fits to the cross-section data using Bayes's equations. The Reich-Moore approximation [28] is used in the code, *i.e.*, neglecting the level-level interference for the capture channels and neglecting the interference between the aggregate capture channel and other channels. The  $R$ -matrix takes the form of

$$R_{cc'} = \sum_{\lambda} \frac{\gamma_{\lambda c} \gamma_{\lambda c'}}{E_{\lambda} - E - i\gamma_{\lambda\gamma}^2}, \quad (1)$$

where, the subscripts  $c$  and  $c'$  represent only particle channels. The sum over  $\lambda$  includes an infinite number of levels (*i.e.*, resonances); for practical purposes this number is of course truncated to a finite value and the effect of the omitted levels approximated either by large distant levels or by a parameterized  $R^{\text{ext}}$  as given in the SAMMY manual. We have neglected the effect of the omitted levels in the analysis since it is very difficult, as we tried, to observe such small effect in the present statistics and energy resolution level.  $E_{\lambda}$  is the resonance energy, and the quantity  $\gamma_{\lambda\gamma}^2$  is called reduced capture width. The gamma width  $\Gamma_{\lambda}^{\gamma}$  is given in terms of the reduced capture width amplitude (or gamma width amplitude)  $\gamma_{\lambda\gamma}$  as  $\Gamma_{\lambda}^{\gamma} = 2\gamma_{\lambda\gamma}^2$ . The particle width is defined as  $\Gamma_{\lambda c} = 2\gamma_{\lambda c}^2 P_{\ell}$ , and  $\gamma_{\lambda c}^2$  is referred to as reduced particle width. Here, we assume that the gamma widths  $\Gamma_{\lambda}^{\gamma}$  are negligible comparing to the particle widths  $\Gamma_{\lambda c}$ . The Coulomb penetrability is given by

$$P_{\ell} = \frac{kR}{(F_{\ell}^2 + G_{\ell}^2)_R}, \quad (2)$$

where  $k$  is the wave number,  $k = \sqrt{2\mu E_{c.m.}}/\hbar$  ( $\mu$  is the reduced mass).  $F_{\ell}$  and  $G_{\ell}$  are the regular and irregular Coulomb functions, respectively. The channel (or interaction) radius is given by  $R = 1.4(A_t^{1/3} + A_p^{1/3})$  fm [16], and  $A_t$ ,  $A_p$  are the mass numbers of the target and projectile, respectively. Actually, the  $R$ -matrix fitting result is not very sensitive to the choice of radius, and the choice of radius has a minor effect on the rather large uncertainties both in the excitation energy and in the width. The fits with all possible spin-parity assignments to the observed resonances have been attempted. The preferred fits are shown in fig. 1, and the  $\chi^2/N$  values are 2.50 and 2.13, respectively. The energy resolution has been taken into account in the fitting curves. The deduced resonant properties,  $J^\pi$  and  $\Gamma_p$ , have been determined and listed in table 1, where the excitation energies are determined by the data at  $\theta_{c.m.} \approx 172^\circ$  due to their better energy resolution and the uncertainties include both systematic and fitted ones; the proton partial widths are obtained by the weighted average of those deduced from both data at  $\theta_{c.m.} \approx 172^\circ, 146^\circ$ . The excitation energies and spin-parities determined before are also listed for comparison. By comparing the level population intensity in the previous experiments [7–9], the probable parity properties (natural or unnatural) are estimated as listed in the 6th column of table 1. The probable spin-parity and transferred  $\ell$  values are recommended based on the natural-or-unnatural property restrictions (see the 8th column in table 1). For instance, the  $R$ -matrix analysis gives  $J^\pi = (1^-, 2^-, 3^-)$  for the 8.51 MeV state, since it proba-



20. J. Görres *et al.*, Phys. Rev. C **51**, 392 (1995).
21. U. Giesen *et al.*, Nucl. Phys. A **567**, 146 (1994).
22. S. Kubono *et al.*, Eur. Phys. J. A **13**, 217 (2002).
23. Y. Yanagisawa *et al.*, Nucl. Instrum. Methods A **539**, 74 (2005).
24. J.J. He *et al.*, Phys. Rev. C **76**, 055802 (2007).
25. S. Kubono, Nucl. Phys. A **693**, 221 (2001).
26. A.M. Lane, R.G. Thomas, Rev. Mod. Phys. **30**, 257 (1958).
27. N.M. Larson, *A Code System for Multilevel R-Matrix Fits to Neutron Data Using Bayes' Equations*, ORNL/TM-9179/R5 (Oct. 2000).
28. W.C. Reich, M.S. Moore, Phys. Rev. **111**, 929 (1958).
29. P.M. Endt, Nucl. Phys. A **633**, 1 (1998).
30. J.J. He *et al.*, in preparation.